Metallomics

Accepted Manuscript

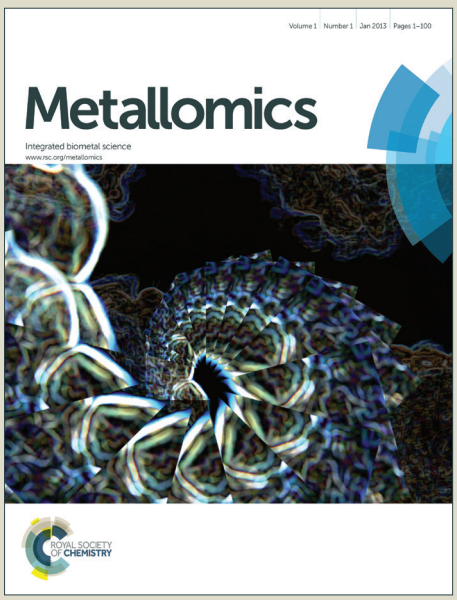

ROYAL SOCIETY OF CHEMISTRY

www.rsc.org/metallomics

Metallomics

Mechanistic evaluation of translocation and physiological impact of titanium dioxide and zinc oxide nanoparticles on the tomato (*Solanum lycopersicum* L.) plant†

Ramesh Raliya[a], Remya Nair[a], Sanmathi Chavalmane[a], Wei-Ning Wang[b,a] and Pratim Biswas[a,*]

[a] Dept. of Energy, Environmental and Chemical Engineering,
Washington University in St. Louis
St. Louis, Missouri -63130, USA

[b] Virginia Commonwealth University, Richmond, Virginia 23284, USA

Revised Manuscript (MT-ART-06-2015-000168.R2)

Submitted to

Metallomics

October 07, 2015

***To whom correspondence should be addressed**

Tel: 314-935-5482

Email: pbiswas@wustl.edu (Biswas)

†Electronic Supplementary Information (ESI)

Mechanistic evaluation of translocation and physiological impact of titanium dioxide and zinc oxide nanoparticles on the tomato (*Solanum lycopersicum* L.) plant†

ABSTRACT: Sustainable use of nanotechnology for agricultural practice requires an understanding of the plant's life cycle and potential toxicological impacts of nanomaterials. The main objective of this study was to compare the impact of TiO_2 and ZnO nanoparticles of similar size (25 ± 3.5 nm) over a range of concentrations (0 to 1000 mg/kg) on translocation and accumulation of nanoparticles in different plant sections; as well as to establish physiological impact on tomato plants. The results indicated that there is a critical concentration of TiO_2 and ZnO nanoparticles upto which the plant's growth and development are promoted; with no improvement beyond that. Aerosol mediated application was found to be more effective than the soil mediated application on the uptake of the nanoparticles was in plants. A mechanistic description of nanoparticle uptake, translocation and resultant plant response is unraveled. The present investigation demonstrates the concept of nanoparticle farming by understanding plant – nanoparticle interaction and biodistribution.

† **Electronic Supplementary Information (ESI) available**: Fig. S1. XRD characterization of TiO2 and ZnO nanoparticles; Fig. S2. PAR absorption by TiO2 NPs treated tomato leaf. The letter T stands for TiO2, and a numeric value with the letter T describes the concentration of TiO2 NPs in mg/Kg; Fig. S3. Effect of TiO2 and ZnO nanoparticles on flower appearance at growth stage on the 40^{th} day after germination; Fig. S4. Effect of TiO2 and ZnO nanoparticles on tomato fruit yield on the 66^{th} day; Fig. S5. Effect of TiO2 and ZnO nanoparticles on dry biomass at the 28^{th} day. The representative figure shows the metal accumulation in the foliar exposure of TiO_2 or ZnO treated plants. Fig.S3-S4, error bar represents the standard deviation. $n = 4$. Asterisk (s) above bar demonstrate significant difference ($p < 0.05$); Table S1: Tomato plant growth stage and phenological analyses. See DOI: 10.1039/x0xx00000x

Introduction

Nanotechnology is an interdisciplinary science related to intentionally created materials with at least one dimension less than 100 nm.[1] These materials are used in a wide range of applications and products due to their unique physicochemical properties.[2] This has also prompted the use of tailor made nanoparticles in fields such as agriculture. The use of nanotechnology has been motivated by the need to feed an expected 9 billion people by 2050; and it is important to explore the intersection of nanotechnology, food, and agriculture as a research priority.[3] For more than a decade, a range of nanoparticles, including carbon, metal, metal-oxide, dendrimers, and composites, have been developed and used in plant science.[4-8] Nanomaterials are generally believed to increase profitability and sustainability,[9] which are essential requirements for improved agricultural production. The preliminary results of increased agricultural use of nanotechnology by densely populated countries such as China and India indicate that this technology might have a great impact on reducing hunger, malnutrition, and child mortality.[7] However, more development is needed before the broader scale use of nanotechnology in the agricultural sector becomes a reality.[3] It has been well established that nanoparticles can penetrate (and be uptaken) and translocate in plants,[6, 10-15] thus suggesting a new nutrient delivery system using nanoscale porous domains for ultimate plant growth and productivity. Delivery pathways of nanomaterials also play an important role in nanoparticle uptake by plant leaves. Wang et al.[10] investigated aerosol-based nanoparticle delivery and transport thorough watermelon leaves. They also noted that aerosolized nanoparticles can be easily applied to leaf surfaces which enter the stomata via gas uptake, avoiding direct interaction with soil systems and reducing potential ecological risks.

In manufacturing industries worldwide, TiO_2 and ZnO nanoparticles are among the 13 most produced and used.[16] Recently these nanoparticles have also been used in agricultural and plant science research, although contradictory results on their benefits are reported. For example, TiO_2 nanoparticles have been incorporated into fertilizers as a photocatalytic bactericide; and to improve crop yield through nitrogen photo-reduction with beneficial physiological responses.[17-21] ZnO nanoparticles have also been used very widely in plant uptake studies with similarly contradictory results. Hernandez-Viezcas et al.[22] reported the translation of Zn from ZnO nanoparticles in soil-grown soybean pods and found that these nanoparticles did not accumulate in the grains, and thus were safe to use as a nutrient. Zhao et al.[23] reported that ZnO nanoparticles had no impact on the growth of cucumber plants, their gas exchange, or chlorophyll content, the same group also investigated the effects of ZnO nanoparticles at 400 and 800 mg/kg of soil on the nutritional properties of cucumber fruits. Sugar content was not affected by any of the above concentrations of ZnO NPs; however, the starch content was increased. Protein fractionation, flavonoid contents, and macronutrients were also not affected by the treatment. Similarly, Wang et al.,[10] examined the uptake and transformation of Zn in various tissues of cowpea (*Vigna unguiculata (L.) Walp*) exposed to ZnO nanoparticles in hydroponic solution and soil culture. ZnO NPs were found to be more toxic in solution culture than in soil culture. In our previous studies,[4-5] biologically synthesized ZnO nanoparticles not only influenced plant growth and development, but also increased the activity of soil enzymes such as phytase, acid phosphatase, and alkaline phosphatase. Thus they enhanced native phosphorous nutrient mobilization in the rhizosphere. In contrast, Lin and Xing[24] found that ZnO nanoparticles reduced the total biomass of ryegrass due to shrunken root tips and highly vacuolated and collapsed root epidermal and cortical cells. Dimkpa et al.[25] also reported

environmental toxicity due to ZnO accumulation in plants.[26-27] Yang and Xing[28] reported that humic-acid-coated TiO_2 and ZnO nanoparticles caused additional environmental toxicity by enhanced absorption of phenanthrene in cultivated soil.

Detailed studies need to be conducted to develop a mechanistic understanding of the various uptake and translocation processes. A paucity of studies in the literature analyzing the effects of such factors as the type of nanoparticles, their size, concentration, mode of delivery, life cycle, and nanoparticle induced physiological and biochemical responses is noted. The present study investigates the impact of TiO_2 and ZnO nanoparticles delivered as either aerosols or by soil application on tomato plants. Uptake, translocation, and phenomenological and biochemical responses were studied for the entire plant life cycle. The lycopene content in ripened fruits was investigated. These detailed studies were used to develop a mechanistic understanding of the various pathways. To the best of our knowledge, this is the first report providing a detailed life cycle assessment of the effects of TiO_2 and ZnO nanoparticles on tomato plants.

Results and discussion

The results for the entire life cycle of the nanoparticles are reported in the following sections. This is followed by a mechanistic evaluation of the various pathways.

Characterization of TiO_2 and ZnO nanoparticles

The size and morphology of the TiO_2 and ZnO nanoparticles were investigated using TEM. Typical TEM micrographs **(Fig. 1 A-B)** revealed that TiO_2 nanoparticles were mostly cubic, whereas ZnO nanoparticles were a mixture of hexagonal and nearly spherical shapes. The geometric mean diameters of the TiO_2 and ZnO nanoparticles were 25±0.64 nm and 28±0.7 nm,

respectively. The insets of Fig. 1A and 1B show the hydrodynamic diameter of TiO_2 and ZnO nanoparticles, respectively, measured by DLS based on particle size distribution (PSD). The electrophoretic zeta potentials of the TiO_2 and ZnO nanoparticles were -22.5±3.4 mV and -29.7 ±5.8 mV, respectively.

The *Bruker DIFFRAC.EVA* program was used to evaluate and process XRD scan data. Both, TiO_2 and ZnO nanoparticles showed peaks that match the characteristic TiO_2 anatase and zincite crystal peaks respectively **(Supplementary Fig. S1)**. Physicochemical characteristics of synthesized nanoparticles are summarized in **Table 1**

Seed germination

Germination tests were carried out as described earlier. Tomato seed germination was not affected by TiO_2 and ZnO nanoparticles in the studied range of concentrations (up to 750 mg/kg). At 1000 mg/kg, germination percentage reached 72.5% and 51.8% for TiO_2 and ZnO nanoparticles, respectively. **Fig. 2** shows the germination rate of tomato seeds after 5^{th} day of treatment with different concentrations of TiO_2 and ZnO nanoparticles.

Growth of tomato plants and exposure to nanoparticles

Tomato plants were grown under controlled conditions for 14 days in separate experiments. The plants were then exposed to TiO_2 and ZnO nanoparticles with soil amended treatment and by aerosol mediated foliar spray on the 14^{th} day of plant growth. Both treatments were carried out with nanoparticle concentrations ranging from 0-1000 mg/kg. On the 28^{th} day of growth the plant height was measured for both modes of treated plants as shown in **Fig. 3.** An increased plant height was observed for TiO_2 and ZnO nanoparticle-treated plants up to 250 mg/kg after using both foliar and soil application methods. For TiO_2 treated plants, further increase in the concentration of nanoparticles did not have significant effect on plant height, particularly for the

soil amended treatment, and the average plant height was highly comparable to the control. On the other hand, plants treated with foliar application of TiO_2 nanoparticles showed significantly decreased root length at all the exposure concentrations except for 1000 mg/kg, where the difference was not statistically significant. Similarly, the root length of soil-treated plants increased significantly up to 250 mg/kg of exposure with nanoparticles, whereas, no significant difference was observed in plants treated with higher concentrations of the nanoparticles.

Compared to the control, ZnO nanoparticle treated plants showed a maximum increase in plant height of 24.5% at 250 mg/kg delivered by soil amended with nanoparticles. With foliar aerosol application, plant height increased by 4.3 to 10.6%. However, the difference was not statistically significant. It was interesting to note that aerosol treated plants showed increased root length up to a 250 mg/kg concentration of the ZnO nanoparticles, and the maximum increase in root length was 49.9% with respect to the controls. Higher concentrations (>250 mg/kg) of ZnO nanoparticles drastically affected the root length of tomato plants in both modes of application.

It is possible that higher concentration of nanoparticles delivered by foliar application could have reached toxic levels in stem and leaves that reduced the plant height. Previous reports on plants such as *Lolium perenne* L and soybean showed decreased plant height in those plants treated by 200 mg/kg and 500 mg/kg ZnO nanoparticles respectively.[29-30] Larue et al.[21] explained that the higher surface reactivity of TiO_2 nanoparticles could enlarge the root pores or create new ones, leading to higher hydro-mineral flow in roots. Subsequently, elevated nutrient uptake might explain the increased root length after treatment with TiO_2 and ZnO nanoparticles. However, more experiments are needed to determine the effects of nanoparticle size and concentration on tomato plant growth.

Chlorophyll content

The chlorophyll content in leaves was measured as an indicator of the plants photosynthetic performance. As can be seen in **Fig. 4**, the relative chlorophyll content in 28-day old tomato plants leaves was increased significantly by both TiO_2 and ZnO nanoparticles delivered by aerosol-foliar and soil application. Plants treated with aerosol-foliar applied TiO_2 nanoparticles showed chlorophyll content increasing from 62.67% to 227.42% for increasing nanoparticle concentrations up to 500 mg/kg. In comparison, plants grown in soil amended with TiO_2 nanoparticles showed a maximum increase in chlorophyll content of 216.29% at a 750 mg/kg nanoparticle concentration with respect to control. Plants similarly treated with ZnO nanoparticles showed a maximum chlorophyll content at 750 mg/kg concentration whereas the aerosol treated plants showed a maximum increment at 1000 mg/kg exposure concentration. Our results are consistent with previous reports. Servin et al.[31] reported that the total chlorophyll content in cucumber leaves increased after treatment with 27 nm mixed phase TiO_2 nanoparticles at a concentration of 750 mg/kg. Our group also observed an increased chlorophyll content in various plant species in response to biologically synthesized TiO_2 and ZnO nanoparticles.[4-5, 19-20, 32]. Chen et al.[33] reported that mixed phase TiO_2 nanoparticles of 21 nm increased the contents of chlorophyll b on a unicellular green alga *Chlamydomonas reinhardtii*. A few contradictory reports were also noted in which chlorophyll content was not affected by treatment with nanoparticles. Such different reports exploited different properties of nanoparticles with different dosages, exposure concentrations, and delivery modes.[34-36] Hence, the fundamental mechanism behind the effects of nanoparticles on photosynthetic pigments is still an open question.

In support of increasing chlorophyll content observed in this study, we also found that on increasing the concentration of TiO_2 nanoparticles in foliar application by aerosol delivery, the absorption of photosynthetically active radiation (PAR) also increased in tomato plant leaves **(Supplementary Fig. S2)**. This indicated that the nanoparticles could help in increasing the rate of plant photosynthesis.

Flower and fruit development

All plants had flowers and fruit at the 40th day of their life cycle **(Supplementary Fig. S3)**. Our observations clearly depicted the importance of the delivery mode rather than the type of nanoparticles on flower development in treated plants. Plants exposed to TiO_2 nanoparticles through aerosol mediated foliar application formed flowers at very low concentrations, while soil treated plants showed an inverse relationship to aerosol treatment, showing a statistically similar number of flowers at higher concentration. Although ZnO nanoparticle treated plants showed an increased number of flowers than control, little statistical difference was noted when comparing the two different modes of nanoparticle application at 250 mg/kg treatment. This provided an indication that foliar application by aerosol method could be used as an effective way to deliver nutrients to plants, and a higher accumulation of nanoparticle may retard plant growth and development.[10, 24, 37]

An overview of the growth stage and phenomenological responses of tomato plants after treatment with TiO_2 and ZnO nanoparticles is given in **Supplementary Table S1**. Several growth stages were measured because of their cumulative effect on yield and nutritional quality of the fruit. Exposure to nanoparticles induced plant growth and development at lower concentrations but decreased at higher concentrations, which might be due to metal oxide induced toxicity.

Fruit yield and nutritional quality

Plants exposed to nanoparticles produced relatively more fruits than the control (**Supplementary Fig. S4**), and the fruits were also relatively bigger and heavier. This is most obvious for 1000 mg/kg soil treated with the TiO_2 and ZnO nanoparticles. Moreover, lower concentration of TiO_2 nanoparticles did not exert any significant effect, whereas ZnO nanoparticles increased fruit yield in both soil and foliar treated plants. On the 66th day, aerosol treated plants produced 81.9% more tomato fruits (by weight) than the control, whereas soil treated plants increased fruit production by 305.4%. By adding up the weight of all tomato fruits of an individual tomato plant regardless of the ripening status, the average yield of a single plant was obtained. Our results and observations are consistent with the earlier reports with other nanoparticles and plants, although no such study has yet been reported for tomato plants in response to TiO_2 and ZnO nanoparticles. Rico et al.[38] and Kole et al.[39] found that CeO and carbon based nanoparticles increased wheat and bitter melon yield by 36.6% and 128%, respectively. Similarly, Wang et al.[34] found that a longer vegetative stage enhanced fruit yield in CeO_2-exposed tomato plants.

Lycopene, an antioxidant, is an important nutritional parameter in tomato fruits. The ripened fruits collected from treated plants, all had an indicated an increase in lycopene content with respect to control plants except for plants exposed to 1000 mg/kg ZnO nanoparticles by foliar application (**Fig. 5**). Overall, it was observed that foliar application induced more lycopene biosynthesis than soil application. Further, the effect also varied with the type of nanoparticle: As shown in **Fig. 5**, the lycopene content was increased by 113.1 % and 80.2% in fruits obtained from plants treated with 100 mg/kg ZnO and TiO_2 nanoparticles by foliar application. The mechanism behind nanoparticle-induced lycopene biosynthesis is still an open

question. A similar observation was found by Kole et al.[39] in bitter melon, in which they found an 82% lycopene content enhancement by application of carbon based fullerol nanoparticles.

Dry biomass yield

Dry biomass collected upon first harvesting on the 28th day of the life cycle exhibited significant variation with respect to the control and nanoparticle-exposed plants (**Supplementary Fig. S5**). The highest increase in biomass yield was from 250 mg/kg TiO_2 nanoparticle aerosol exposure, which led to an increase of 69.6% over the control. It was followed by 100 mg/kg ZnO exposed by soil mode, which was at par and resulted in an increase of 40.7% over the control. Foliar application of TiO_2 and ZnO nanoparticles at a concentration of 1000 mg/kg reduced biomass by 6.8% and 10.9%, respectively, over the control. The increased biomass content could be correlated with the effects observed on chlorophyll content and photosynthetically active radiation.

Increased light absorption by plant leaves could ultimately lead to enhanced biomass. Interestingly, it was also noted that 1000 mg/kg TiO_2 nanoparticle treatment produced an increase in chlorophyll content but reduced total biomass. It is speculated that nanoparticles boosted plant growth at a critical growth period, but their subsequent accumulation caused metal-induced toxicity. Many researchers have also reported that nanoparticles enhance plant biomass, but the mechanism behind the plant biomass increment[5, 20, 32, 34, 38-40] has not yet been determined. A comprehensive review article by Rico et al.[41] listed several nanoparticles as having positive, non-consequential, or negative effects on different food crops, which further corroborated our observations. Our study demonstrated the varying effects on a single plant species by different types of same sized nanoparticles through aerosol based foliar application and soil exposure methods.

Distribution and accumulation of Ti and Zn among plant tissues

The distribution of nanoparticles in plants, including their edible parts, is a food safety concern. Ti and Zn concentration in dried tomato plant tissues are shown in **Fig. 6**. The ICP-MS data, normalized to the control plants, showed the presence of Ti and Zn in stem, roots, leaves, and fruits of tomato plants exposed to TiO_2 and ZnO nanoparticles. Here in, data of one concentration with the same particle size and mode of application showed different degrees of metal accumulation. **Fig. 6** clearly shows that the 250 mg/kg concentration of TiO_2 nanoparticles accumulates more in the stem, whereas ZnO nanoparticles accumulate more in the leaves. However, Zn accumulated more in the leaves when applied by the foliar mode, while Ti showed a maximum accumulation with soil application. Similarly, ICP-MS analyses showed metal accumulation in fruits treated with different concentrations of TiO_2 and ZnO nanoparticles, but the accumulations were not statistically significant. The concentration of Ti in tomato plant tissues followed the sequence stem>roots>leaves>fruits independent of exposure method, and similar observations were recorded for ZnO exposed by soil application. However, aerosol exposed ZnO nanoparticles showed maximum Zn concentrations in the sequence leaves>roots>stems>fruits. It is reported that both metal oxide and metal ions are difficult to translocate into plant stem, and only a small percentage translocate from root to stems[23, 35, 42]. Results of soil-treated nanoparticles are consistent with these earlier reports on different plant types and tissues. However, aerosol foliar application provided evidence that biodistribution of nanoparticles depends not only on nanoparticle type but also on the mode of exposure. An increase in metal ion accumulation was observed in the leaves with an increase in both TiO_2 and ZnO nanoparticle exposure concentrations (**Fig. 7**). However, in cases of TiO_2 nanoparticle exposure, inconsistent trends were observed for root tissues.

Plant anatomical studies using TEM confirmed that the nanoparticles maintained their morphology even after interaction with biological tissues. TEM observation from different plant parts **(Fig. 8)** showed that the accumulated particles had remained in nanoscale, even up to the fruiting stage. Several reports in the literature also showed the presence of different metal nanoscale particles, such as CeO, ZnO, MgO, and Fe_2O_3, in different plants parts at various growth stages.[10-11, 24, 39, 41] Such bioaccumulation of engineered nanoparticles may impact the food chain and food web. Therefore, further fundamental investigation with respect to nanoparticle–plant interactions, the factors responsible for accumulation in plant tissues, and their effects on rhizospheric microbial community structure are needed to ensure precision agricultural application of nanotechnology.

Mechanistic description: uptake, translocation and plant response

Figure 8 illustrates the mechanistic pathways of the nanoparticle uptake, accumulation and responses in the tomato plant. The uptake of metal oxide nanoparticles depends on plant species, plant age, and nanoparticle properties such as morphology and surface functionalization.[6, 41] In addition, nanoparticle (independent of being a metal, metal oxide or carbon based origin) uptake depends on exposure pathways, co-related with the physiological and metabolic responses of the plant. In this study, ICP-MS **(Fig. 6)** and TEM (**Fig. 8)** results revealed that nanoparticles were accumulated in roots, shoots and leaves; independent of the application methodology. This clearly indicates that once nanoparticles are uptaken by tomato plants (either through root cell or leaf cell), they are bio-distributed throughout the plant by its vascular system. Nanoparticles uptaken by leaf cells are transported by phloem (bi-directional pathways). Previous studies suggested that foliar application of nanoparticles can enter into plant cells by gas uptake mechanisms, either as an aerosol or by direct penetration to cells because of their small

size.[43] Soil mediated nanoparticles up-taken by root cells are transported by the xylem through unidirectional pathways, along with water. Nanoparticles applied to the soil, first undergo biotransformation by humic acid and root exudates, and this is followed by uptake by surface pores of roots.[41] In addition, smaller nanoparticles create new root pores due to their higher surface reactivity, resulting in an increase in hydro-mineral flow and nutrient uptake.[44] However, the accumulation rate in tissue is different for both foliar and soil application. A more detailed investigation is needed to confirm these pathways responsible for aerosol-gaseous uptake and biotransformation.

In the range of concentrations (0 to1000 mg/kg) of the nanoparticles tested, they either had an inconsequential or a slightly enhancing effect on tomato growth and development. Once TiO_2 is uptaken by the tomato plant, it functions as a nutritional non-essential element. The observed trends are due to the enhanced light absorbtion of TiO_2 and chlorophyll content in the plant.[45] The essential role of TiO_2 as a plant nutrient is still a debatable point. In contrast, zinc is an essential micronutrient, and is often supplied as zinc sulfate in agricultural practice to overcome Zn deficiency in plants. Zn acts as a cofactor for a number of metabolic and physiological cycles. ZnO nanoparticles increase activity of phosphorous mobilizing enzymes such as phosphatase and phytase in the rhizosphere, thus increasing the phosphorous availability to plants.[4] Hence the enhanced physiological and biochemical response is consistent with a twin role as an essential nutrient and mobilizer of native phosphorous.

Experimental

The experimental plan is summarized in **Table 2**. The primary objective was to study engineered TiO_2 and ZnO nanoparticle impact on phenological and biochemical characteristics

of tomato plants throughout their life cycle (from germination to fruit ripening stage). In addition, the nutritional value of a specific tomato fruit and the transport of nanoparticles were also assessed. Details of the experimental plan are described in the following sections.

Plant material

Tomato (*Solanum lycopersicum* L.), is an important agricultural and medicinal plant, grown worldwide and consumed in diverse ways. The fruit is rich in lycopene, one of the most powerful natural antioxidants, which protects against epidemiological oxidative damage and several chronic diseases, including cancer.[46-48] For this study, we selected a hybrid variety, "tomato cherry super sweet 100". Seeds were purchased from Main Street Seed and Supply, Bay City, MI, USA.

Synthesis of TiO_2 and ZnO nanoparticles

TiO_2 nanoparticles were prepared by hydrothermal reaction of titanium alkoxide stabilized in acidic ethanol/water solution as reported elsewhere.[49] In brief, 0.02 M titanium isopropoxide (97% Sigma Aldrich, MO, USA) was mixed in 1:8 ethanol/water with stirring. The solution pH was adjusted to 0.7 by adding nitric acid. After 4 h of stirring, the solution was subjected to hydrothermal reaction at 240 °C for 4 h without stirring. After hydrothermal reaction, the crystallized TiO_2 nanoparticles were obtained as a colloidal suspension.

ZnO nanoparticles were synthesized by the sol–gel method described by Zak et al.[50] In brief, 11.2 g of $Zn(NO_3)_2 \cdot 6H_2O$ was dissolved in 25 ml of deionized (DI) water and then stirred for 30 min. Meanwhile, 5 g of starch was dissolved in 75 ml of DI water and stirred for 30 min at 75 °C, followed by the addition of the $Zn(NO_3)_2 \cdot 6H_2O$ solution. The mixture was then incubated for 10 h at 80 °C with stirring. The obtained powder was calcined at 500 °C for 5 h to obtain ZnO nanoparticles.

Characterization of TiO_2 and ZnO nanoparticles

The diameter of the synthesized nanoparticles was determined by transmission electron microscopy (TEM, FEI Technai G2 Spirit), and the hydrodynamic diameter and zeta potential were determined by dynamic light scattering (DLS, Malvern). The crystal phase of the nanoparticles was assessed by X-ray diffraction (XRD, Bruker D8 Advance) using CuKα radiation.

Preparation of exposure suspension

Suspensions of TiO_2 and ZnO nanoparticles were prepared right before exposure at particle concentration of 0 (control), 10, 100, 250, 500, 750 and 1000 mg/kg in DI water and sonicated for 30 minutes. The pH of each suspension was adjusted by 0.1N HCl and NaOH to 6.8±0.3 before plant exposure.

Seed germination test

To avoid surface contamination of seeds used to test the impact of nanoparticles on germination, seeds were first soaked in 2.5% NaClO for 15 minutes, then in ETOH for 10 min. and finally in sterilized DI water. Air dried seeds were soaked for 1 h in nanoparticle suspensions, prepared as described above, under static condition. Seeds were then transferred to petri dishes with wet filter paper and kept in darkness. There were 10 seeds for each treatment. After 5 days, the germination percentage was calculated based on the emergence of radicle and plumule.

Foliar and root exposure to nanoparticles

In the present study, nanoparticles were applied to plants by foliar or root exposure. Foliar application was made on 14–day-old plants grown in a greenhouse (as explained in the next section) by aerosol exposure using an atomizer nozzle equipped with peristaltic pump. For root exposure, suspensions of ZnO or TiO_2 nanoparticles (prepared as described in the previous

section) were amended individually with 100% calcined fullers earth (TURFACE® MVP®, J. R. Peters, Inc.) in plastic pots (20 cm × 18 cm). Potted soil without any nanoparticle treatment was kept as a control, and there were four replicates for each treatment. All the pots were allowed to equilibrate for 24 hours before sowing the tomato seeds.

Tomato plant growth and greenhouse conditions

Four tomato seeds were sowed in each pot. The germinated seedlings were grown for 66 days in a controlled environment in a USDA approved plant growth facility center at Washington University in St. Louis. The temperature in the growth facility was maintained at 30±3 ºC (mean ± standard deviation) during the day and 25±2 ºC at night. The daily light integral (photosynthetic active radiation) was 20±2.6 mol. $m^{-2}d^{-1}$. In addition, alternate day watering with basal nutrient solution was provided in equal amounts to each pot.

During the entire life cycle of the tomato plants, physiological parameters, such as plant height, root length, and each plant's dry biomass and biochemical parameters, such as chlorophyll content, were recorded on the 28th day after germination. Flowering and fruit appearance was recorded at the 40th day, and fruit yield, the lycopene content in the tomato fruit, and elemental analyses were recorded on the 66th day of the plant's life cycle. Total fruit yield was calculated as cumulative harvest from the 50th day to the 66th day.

Chlorophyll estimation

To measure the chlorophyll content, one third of the plant leaves were collected on the 28th day and washed with tap water followed by DI water. 1 g of fresh plant leaves were cut into small pieces and dipped in absolute acetone for 12 hours under dark. After incubation, the extracted chlorophyll was recorded spectro-photometrically at 661.6 nm, 664.8 nm and 470 nm

wavelength. Total chlorophyll content was calculated according to the formula described elsewhere.[51]

Lycopene measurement in tomato fruit

Lycopene, the predominant carotenoid in tomato red fruits, exhibits high antioxidant activity. Therefore, the lycopene content of the freshly harvested ripe tomato fruits was estimated according to the method suggested by the Food and Agriculture Organization.[52]

Elemental analyses

Elemental analyses were used to investigate nanoparticle mobilization and accumulation in the plant parts, including the fruits. The concentrations of Ti and Zn in the leaf, stem, root, and ripened tomato fruits were detected by an inductively coupled plasma mass spectrometer (ICP-MS, ELAN DRC II, Perkin Elmer Inc.). The plant samples were initially dried, weighed and placed in a 20 ml glass vial and then digested using 5 ml of HNO_3 and 1 ml of hydrogen peroxide at a temperature of 150 °C until the solution turned clear and the solution was then evaporated till it reached to 1 ml. The completely digested samples were diluted by 2 ml of 1% nitric acid and then filtered using 0.2 µm nylon filter, followed by a 0.02 µm membrane filter (Whatman inorganic membrane filter). The final filtered solution was again diluted by a factor of three before analysis by ICP-MS.

Plant anatomy

To determine the penetration and determination of nanoparticles, anatomical studies of plant parts were carried out by using different techniques[6], such as light microscopy, fluorescence microscopy, and electron microscopy. In the present study, plant samples were collected on the 28th day after nanoparticle application. Small pieces of plant tissue were immersed in 2.5% phosphate buffered glutaraldehyde for 4 h. The plant tissues were then rinsed with 0.1M

phosphate buffer three times and subjected to secondary fixation using 2% osmium tetroxide for 3 h followed by dehydration in a series of five ethanol washes. The tissues were then infiltrated with a mixture of epoxy resin and propylene oxide as a transitional solvent, followed by complete infiltration with resin. Finally the resin was polymerized in oven at 600 °C and the of plant tissues were ultra-sectioned with a thickness of 70 nm using a ultramicrotome (Leica, USA), followed by staining of sections with 4% uranyl acetate before imaging using TEM (FEI Tecnai G2 Spirit) at 120 KV.

Statistical analyses

The results were expressed as mean ± SD (standard deviation). *n=4*. Statistical analyses was performed using data analyses function of Microsoft Excel V.2013. The significant difference in the same concentration of TiO_2 or ZnO nanoparticle exposure were analyzed by Student T-test. A *p*-value of less than 0.05 ($p < 0.05$) was considered as statistically significant.

Conclusions

In summary, the results revealed that aerosol- and soil-mediated exposure of TiO_2 and ZnO nanoparticles led to varying effects on plant phenology, fruit and biomass yield, nutritional quality, and chlorophyll contents. Once the nanoparticles are up taken by the plant, they are bio-distributed through the entire plant by the vascular network. However, the accumulation rate in tissue is different for foliar and soil application. Independent of nanoparticle type, a concentration of 250 mg/kg of TiO_2 and ZnO nanoparticles promoted the highest plant height, root length, and biomass. Lycopene content and fruit yield were a maximum for 100 mg/kg exposure of nanoparticles, whereas 750 mg/kg of nanoparticles led to increased chlorophyll content. TiO_2 nanoparticles increased the light absorption and chlorophyll content in the plant.

Zinc oxide nanoparticles had a twin role of being an essential nutrient and a co-factor for nutrient mobilizing enzymes. Selecting the proper concentration of nanoparticles is important for realizing higher benefits for a target agro-economic trait.

Acknowledgments

We thank Mike Dyer of the Plant Growth Facility Center, Department of Biology, Washington University in St. Louis, for providing space and their support to maintain plants. Partial support by the Lopata Endowment is gratefully acknowledged. This work was performed in part at the Nano Research Facility (NRF) of Washington University in St. Louis. This research facility is a member of the National Nanotechnology Infrastructure Network (NNIN) supported by the National Science Foundation under Grant No. ECS-0335765.

Notes

The authors declare no competing financial interest.

References

1. P. Biswas, An, W.-J., and Wang W.-N. , in *Nature's Nanostructures*, ed. A. B. a. H. Guo. Pan Stanford Publishing: Singapore, 2012, pp 443-476.
2. J. Jiang, G. Oberdorster, A. Elder, R. Gelein, P. Mercer, P. Biswas, *Nanotoxicol.*, 2008, **2**, 33-42.
3. H. Chen, J. N. Seiber, M. Hotze, *J. Agric. Food. Chem.*, 2014, **62**, 1209-1212.
4. R. Raliya, J. C. Tarafdar, *Agri. Res.*, 2013, **2**, 48-57.
5. J. C. Tarafdar, R. Raliya, H. Mahawar, I. Rathore, *Agri. Res.*, 2014, **3**, 257-262.
6. R. Nair, S. H. Varghese, B. G. Nair, T. Maekawa, Y. Yoshida, D. S. Kumar, *Plant Sci.*, 2010, **179**, 154-163.
7. A. Gogos, K. Knauer, T. D. Bucheli, *J. Agric. Food. Chem.*, 2012, **60**, 9781-9792.
8. L. R. Khot, S. Sankaran, J. M. Maja, R. Ehsani, E. W. Schuster, *Crop Protection*, 2012, **35**, 64-70.
9. C. Som, M. Berges, Q. Chaudhry, M. Dusinska, T. F. Fernandes, S. I. Olsen, B. Nowack, *Toxicology*, 2010, **269**, 160-169.
10. P. Wang, N. W. Menzies, E. Lombi, B. A. McKenna, B. Johannessen, C. J. Glover, P. Kappen, P. M. Kopittke, *Environ. Sci. Technol.*, 2013, **47**, 13822-13830.
11. M. Khodakovskaya, E. Dervishi, M. Mahmood, Y. Xu, Z. Li, F. Watanabe, A. S. Biris, *ACS Nano*, 2009, **3**, 3221-3227.
12. X. Ma, J. Geiser-Lee, Y. Deng, A. Kolmakov, *Sci. Total Environ.*, 2010, **408**, 3053-3061.
13. H. Zhu, J. Han, J. Q. Xiao, Y. Jin, *J. Environ. Monit.*, 2008, **10**, 713-717.
14. Z.-J. Zhu, H. Wang, B. Yan, H. Zheng, Y. Jiang, O. R. Miranda, V. M. Rotello, B. Xing, R. W. Vachet, *Environ. Sci. Technol.*, 2012, **46**, 12391-12398.

15. L. Zhao, J. R. Peralta-Videa, M. Ren, A. Varela-Ramirez, C. Li, J. A. Hernandez-Viezcas, R. J. Aguilera, J. L. Gardea-Torresdey, *Chem. Eng. J.*, 2012, **184**, 1-8.

16. OECD, *Organisation for Economic Co-operation and Development Report*, 2010, 1-16.

17. F. Yang, C. Liu, F. Gao, M. Su, X. Wu, L. Zheng, F. Hong, P. Yang, *Biol. Trace Elem. Res.*, 2007, **119**, 77-88.

18. L. Zheng, F. Hong, S. Lu, C. Liu, *Biol. Trace Elem. Res.*, 2005, **104**, 83-91.

19. A. Tarafdar, R. Raliya, W.-N. Wang, P. Biswas, J. C. Tarafdar, *Adv. Sci., Eng. Med.*, 2013, **5**, 943-949.

20. R. Raliya, Biswas, P., Tarafdar, J. C., *Biotechnol. Rep.*, 2015, **5**, 22-26.

21. C. Larue, G. Veronesi, A.-M. Flank, S. Surble, N. Herlin-Boime, M. Carrière, *J. Toxicol.Environ.l Health, Part A*, 2012, **75**, 722-734.

22. J. A. Hernandez-Viezcas, H. Castillo-Michel, J. C. Andrews, M. Cotte, C. Rico, J. R. Peralta-Videa, Y. Ge, J. H. Priester, P. A. Holden, J. L. Gardea-Torresdey, *ACS Nano*, 2013, **7**, 1415-1423.

23. L. Zhao, Y. Sun, J. A. Hernandez-Viezcas, A. D. Servin, J. Hong, G. Niu, J. R. Peralta-Videa, M. Duarte-Gardea, J. L. Gardea-Torresdey, *J. Agric. Food. Chem.*, 2013, **61**, 11945-11951.

24. D. Lin, B. Xing, *Environ. Sci. Technol.*, 2008, **42**, 5580-5585.

25. C. O. Dimkpa, D. E. Latta, J. E. McLean, D. W. Britt, M. I. Boyanov, A. J. Anderson, *Environ. Sci. Technol.*, 2013, **47**, 4734-4742.

26. M. A. Maurer-Jones, I. L. Gunsolus, C. J. Murphy, C. L. Haynes, *Anal. Chem.*, 2013, **85**, 3036-3049.

27. R. Brayner, S. A. Dahoumane, C. Yéprémian, C. Djediat, M. l. Meyer, A. Couté, F. Fiévet, *Langmuir*, 2010, **26**, 6522-6528.

28. K. Yang, B. Xing, *Environ. Sci. Technol.*, 2009, **43**, 1845-1851.

29. M. Bonnet, O. Camares, P. Veisseire, *J. Exp. Bot.*, 2000, **51**, 945-953.

30. J. H. Priester, Y. Ge, R. E. Mielke, A. M. Horst, S. C. Moritz, K. Espinosa, J. Gelb, S. L. Walker, R. M. Nisbet, Y.-J. An, *Proc. Nat. Acad. Sci.*, 2012, **109**, E2451-E2456.

31. A. D. Servin, M. I. Morales, H. Castillo-Michel, J. A. Hernandez-Viezcas, B. Munoz, L. Zhao, J. E. Nunez, J. R. Peralta-Videa, J. L. Gardea-Torresdey, *Environ. Sci. Technol.*, 2013, **47**, 11592-11598.

32. R. Raliya, J. C. Tarafdar, S. Singh, R. Gautam, K. Choudhary, V. G. Maurino, V. Saharan, *Adv. Sci., Eng. Med.*, 2014, **6**, 538-545.

33. L. Chen, L. Zhou, Y. Liu, S. Deng, H. Wu, G. Wang, *Ecotoxicol. Environ.l Safety*, 2012, **84**, 155-162.

34. Q. Wang, X. Ma, W. Zhang, H. Pei, Y. Chen, *Metallomics*, 2012, **4**, 1105-1112.

35. A. Mukherjee, J. R. Peralta-Videa, S. Bandyopadhyay, C. M. Rico, L. Zhao, J. L. Gardea-Torresdey, *Metallomics*, 2014, **6**, 132-138.

36. U. Song, H. Jun, B. Waldman, J. Roh, Y. Kim, J. Yi, E. J. Lee, *Ecotoxicol. Environ.l Safety*, 2013, **93**, 60-67.

37. W. Du, Y. Sun, R. Ji, J. Zhu, J. Wu, H. Guo, *J. Environ. Monit.*, 2011, **13**, 822-828.

38. C. M. Rico, S. C. Lee, R. Rubenecia, A. Mukherjee, J. Hong, J. R. Peralta-Videa, J. L. Gardea-Torresdey, *J. Agric. Food. Chem.*, 2014, **62**, 9669-9675.

39. C. Kole, P. Kole, K. M. Randunu, P. Choudhary, R. Podila, P. C. Ke, A. M. Rao, R. K. Marcus, *BMC biotechnol.*, 2013, **13**, 37.

40. R. Sheykhbaglou, M. Sedghi, M. T. Shishevan, R. S. Sharifi, *Notulae Scientia Biologicae*, 2010, **2**, 112-113.

41. C. M. Rico, S. Majumdar, M. Duarte-Gardea, J. R. Peralta-Videa, J. L. Gardea-Torresdey, *J. Agric. Food. Chem.*, 2011, **59**, 3485-3498.

42. L. Zhao, J. R. Peralta-Videa, C. M. Rico, J. A. Hernandez-Viezcas, Y. Sun, G. Niu, A. Servin, J. E. Nunez, M. Duarte-Gardea, J. L. Gardea-Torresdey, *J. Agric. Food. Chem.*, 2014, **62**, 2752-2759.

43. W. N. Wang, J. C. Tarafdar, P. Biswas, *J. Nanopart. Res.*, 2013, **15**, 151417.

44. M. Ruffini Castiglione, L. Giorgetti, C. Geri, R. Cremonini, *J. Nanopart. Res.*, 2011, **13**, 2443-2449.

45. V. B. Shah, W. R. Henson, T. S. Chadha, G. Lakin, H. Liu, R. E. Blankenship, P. Biswas, *Langmuir*, 2015, **31**, 1675-1682.

46. S. Agarwal, A. V. Rao, *Can. Med. Assoc. J.*, 2000, **163**, 739-744.

47. P. Palozza, A. Catalano, M. Zaccardi, in *Cancer Chemoprevention and Treatment by Diet Therapy*. Springer, 2013, pp 141-167.

48. A. Rao, S. Agarwal, *Nutrit. Res.*, 1999, **19**, 305-323.

49. S. Y. Chae, M. K. Park, S. K. Lee, T. Y. Kim, S. K. Kim, W. I. Lee, *Chem. Mater.*, 2003, **15**, 3326-3331.

50. G. S. Irmukhametova, G. A. Mun, V. V. Khutoryanskiy, *Langmuir*, 2011, **27**, 9551-9556.

51. H. K. Lichtenthaler, *J. Plant Physiol.*, 1987, **131**, 101-110.

52. FAO, *http://www.fao.org/ag/agn/jecfa-additives/specs/monograph7/additive-517-m7.pdf*, 2009 (Access on April 21. 2015).

LIST OF FIGURES

Fig. 1: Morphological characterization of synthesized nanoparticles (A) TEM image of TiO_2 nanoparticles. Inset: hydrodynamic diameter and particle size distribution for TiO_2 nanoparticles measured by DLS. (B) TEM image of ZnO nanoparticles. Inset: hydrodynamic diameter and particle size distribution for ZnO nanoparticles measured by DLS.

Fig. 2. Germination of tomato seeds after treatment with different concentrations of TiO_2 and ZnO. Error bar represents the standard deviation. $n = 4$.

Fig. 3. Effect of TiO_2 and ZnO nanoparticles on plant height and root length of tomato after 28^{th} day of germination. (*Plant height and root length were considered as a phenological character).* Error bar represents the standard deviation. $n = 4$. Asterisk(s) above bar demonstrate significant difference ($p < 0.05$).

Fig. 4. Effects of TiO_2 and ZnO nanoparticles on chlorophyll contents in the leaves of 28-day old tomato plants. Error bar represents the standard deviation. $n = 4$. Asterisk(s) above bar demonstrate significant difference ($p < 0.05$).

Fig. 5. Effect of TiO_2 and ZnO nanoparticles on lycopene content in tomato fruit. Error bar represents the standard deviation. $n = 4$. Asterisk(s) above bar demonstrate significant difference ($p < 0.05$).

Fig. 6. Mobilization and accumulation of Ti and Zn among plant parts: accumulation of metal ion in stems, roots and leaves. Error bar represents the standard deviation. $n = 4$. Asterisk(s) above bar demonstrate significant difference ($p < 0.05$).

Fig. 7. Dose response changes in the concentration of Ti or Zn in the shoot, root and leaves at plant maturity stage. The representative figure shows the metal accumulation in the foliar exposure of TiO_2 or ZnO treated plants. Error bar represents the standard deviation. $n = 4$. Asterisk (s) above bar demonstrate significant difference ($p < 0.05$).

Fig. 8. Mechanistic understanding of nanoparticle uptake, translocation and accumulation helps explain change in tomato's physiological and biochemical responses. TEM micrograph of leaf (A) and stem (B) shows foliar application of TiO_2 nanoparticles accumulation and translocation. Scale bar of inset A and B corresponds to 1 μ and magnified micrograph scale corresponds to 20 nm.

LIST OF TABLES

Tables

Table 1: Physico-chemical characteristic of nanoparticles.

Nanoparticle	Geometric mean diameter (nm)	Mean hydrodynamic diameter (nm)*	Zeta potential (mV)**	Crystal nature
TiO_2	25±0.64	37±6.2	-22.5±3.4	Anatase
ZnO	28±0.7	52±4.3	-29.7±5.8	Zincite

*based on number distribution

**nanoparticles dispersed in DI water

Table 2: Summary of experimental plan for aerosol-based foliar and soil amended TiO_2 and ZnO nanoparticle delivery (Exposure concentration 0-1000 mg/kg).

Experiment #	Method	Parameters quantified (or Technique used)	Objectives
1	Sol gel and hydrothermal method of nanoparticle synthesis	TEM	Physical diameter of nanoparticle
		DLS	Hydrodynamic diameter, size distribution and zeta potential of nanoparticles
		XRD	Crystal nature of nanoparticles
	Nanoparticle suspension	In water using sonication	To be aerosolized or amended in soil for plant exposure or delivery
2	Seed germination	Germination index	To study impact of nano-particles on induction of germination
3	Nanoparticle delivery to plant	Aerosol delivery for foliar application and amended with soil for root exposure	To study comparative assessment of delivery approach through life cycle
4	Phenological study	Plant height, root length, dry biomass, flower and fruit appearance, fruit yield	To determine physiological impact
5	Biochemical study	Chlorophyll content, PAR absorption, lycopene content in the fruit	To determine biochemical and nutritional content in edible fruits
6	Nanoparticle transport and accumulation	TEM and ICP-MS analyses	To study distribution of nanoparticles in plant tissues

TOC GRAPHIC

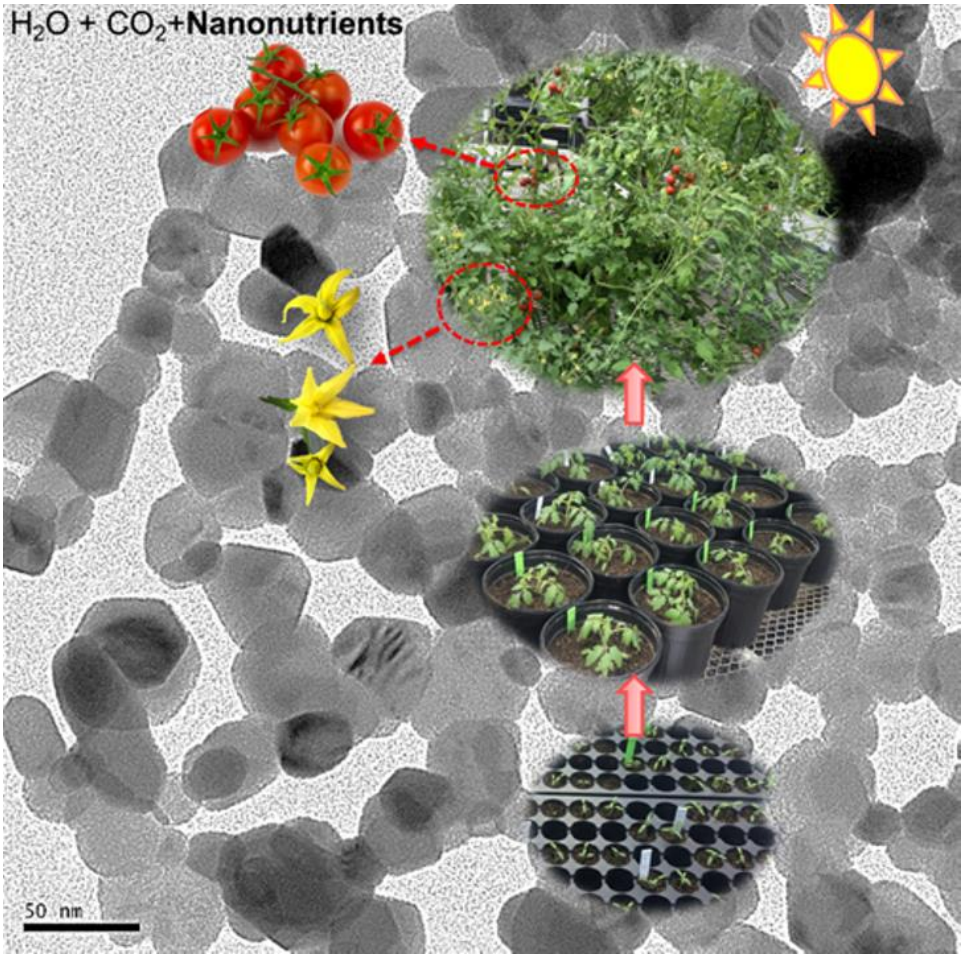

TOC Graphic: Nanonutrient for enhanced crop production and increased solar light absorption

Figures

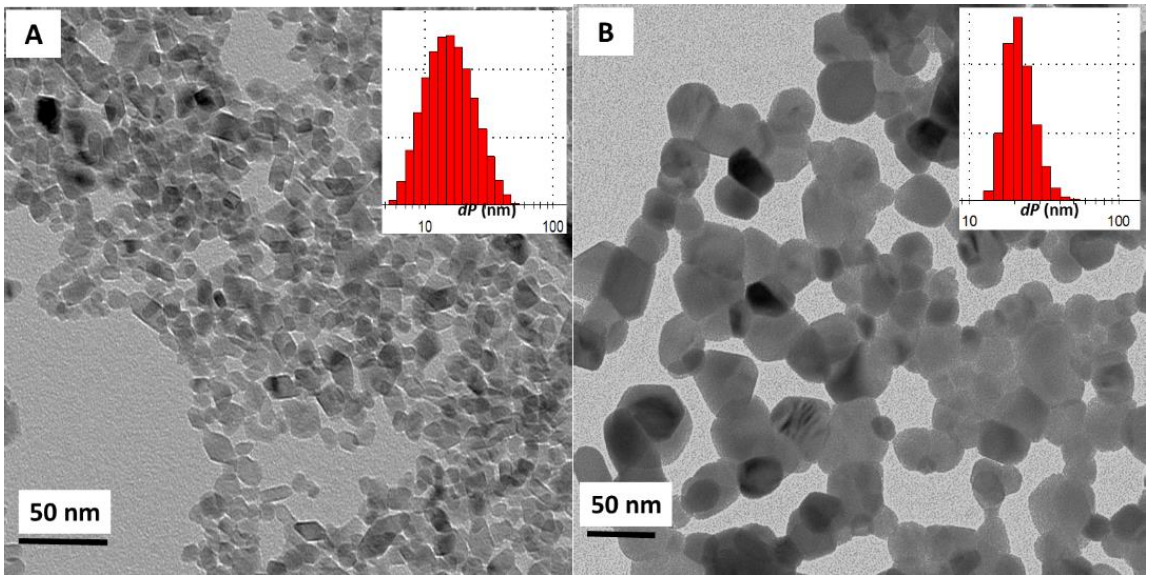

Fig. 1: Morphological characterization of synthesized nanoparticles (A) TEM image of TiO_2 nanoparticles. Inset: hydrodynamic diameter and particle size distribution for TiO_2 nanoparticles measured by DLS. (B) TEM image of ZnO nanoparticles. Inset: hydrodynamic diameter and particle size distribution for ZnO nanoparticles measured by DLS.

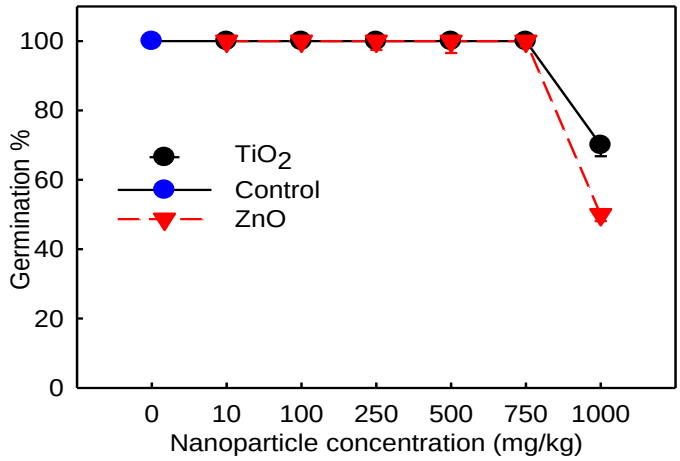

Fig. 2. Germination of tomato seeds after treatment with different concentrations of TiO_2 and ZnO. Error bar represents the standard deviation. *n = 4*.

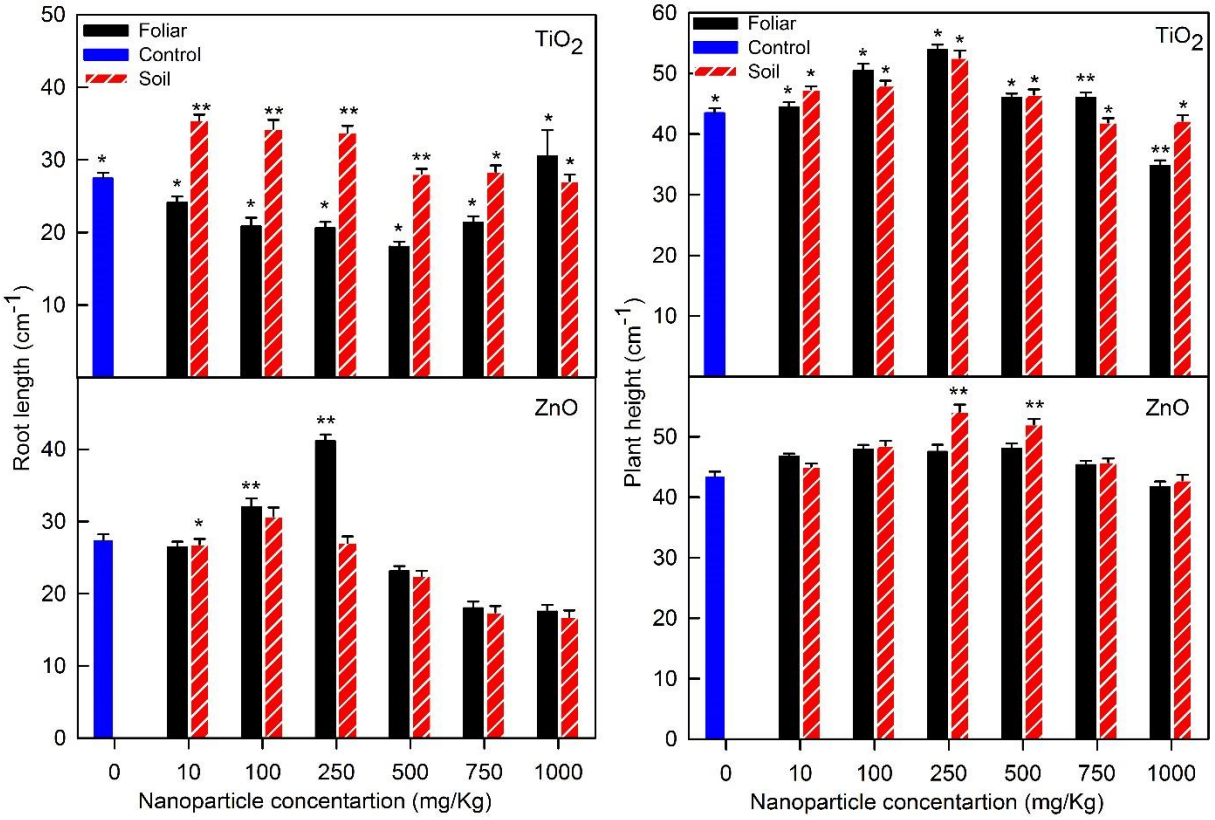

Fig. 3. Effect of TiO_2 and ZnO nanoparticles on plant height and root length of tomato after 28th day of germination. (*Plant height and root length were considered as a phenological character).* Error bar represents the standard deviation. *n = 4*. Asterisk(s) above bar demonstrate significant difference ($p < 0.05$).

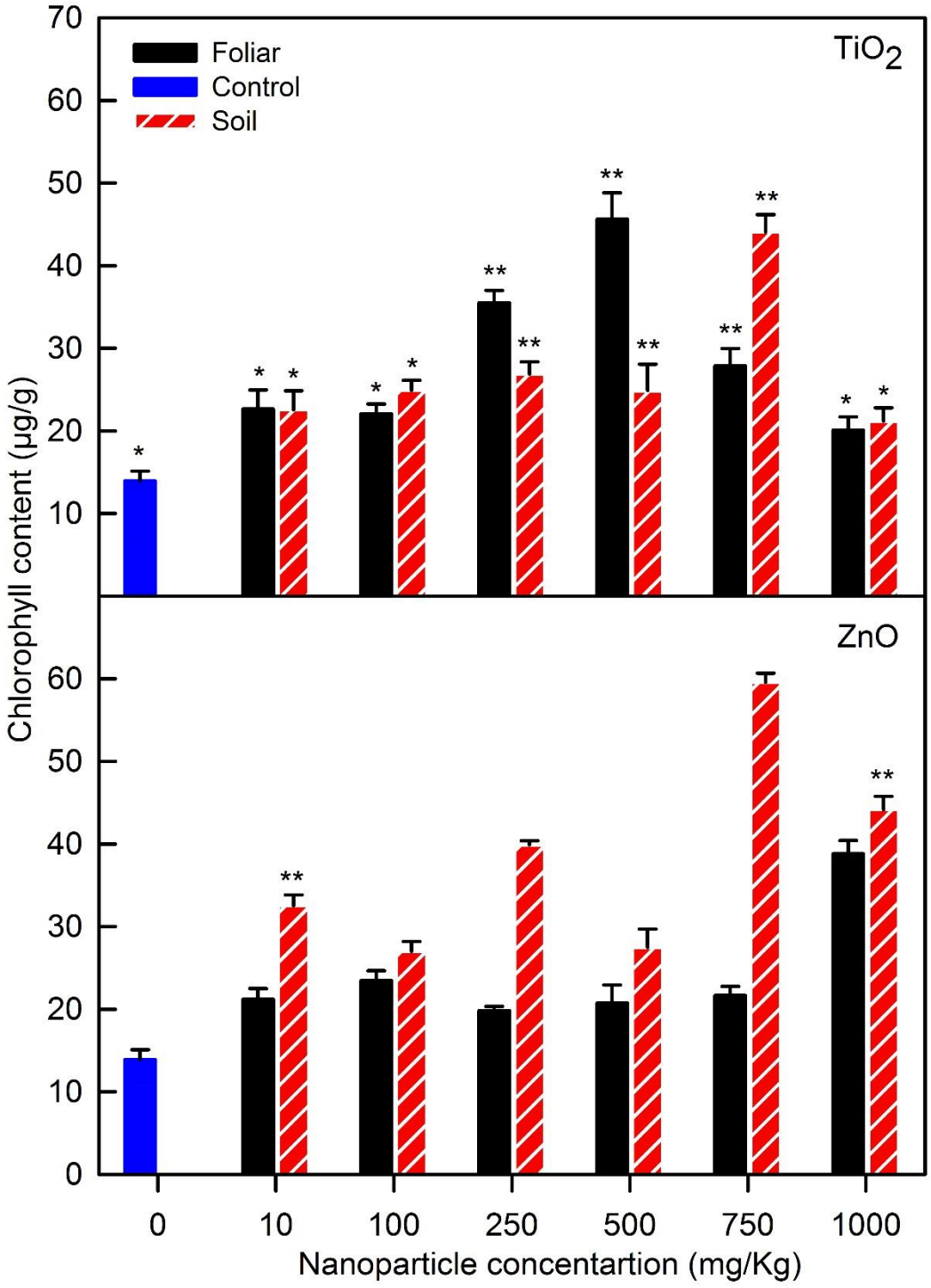

Fig. 4. Effects of TiO_2 and ZnO nanoparticles on chlorophyll contents in the leaves of 28-day old tomato plants. Error bar represents the standard deviation. *n = 4*. Asterisk(s) above bar demonstrate significant difference ($p < 0.05$).

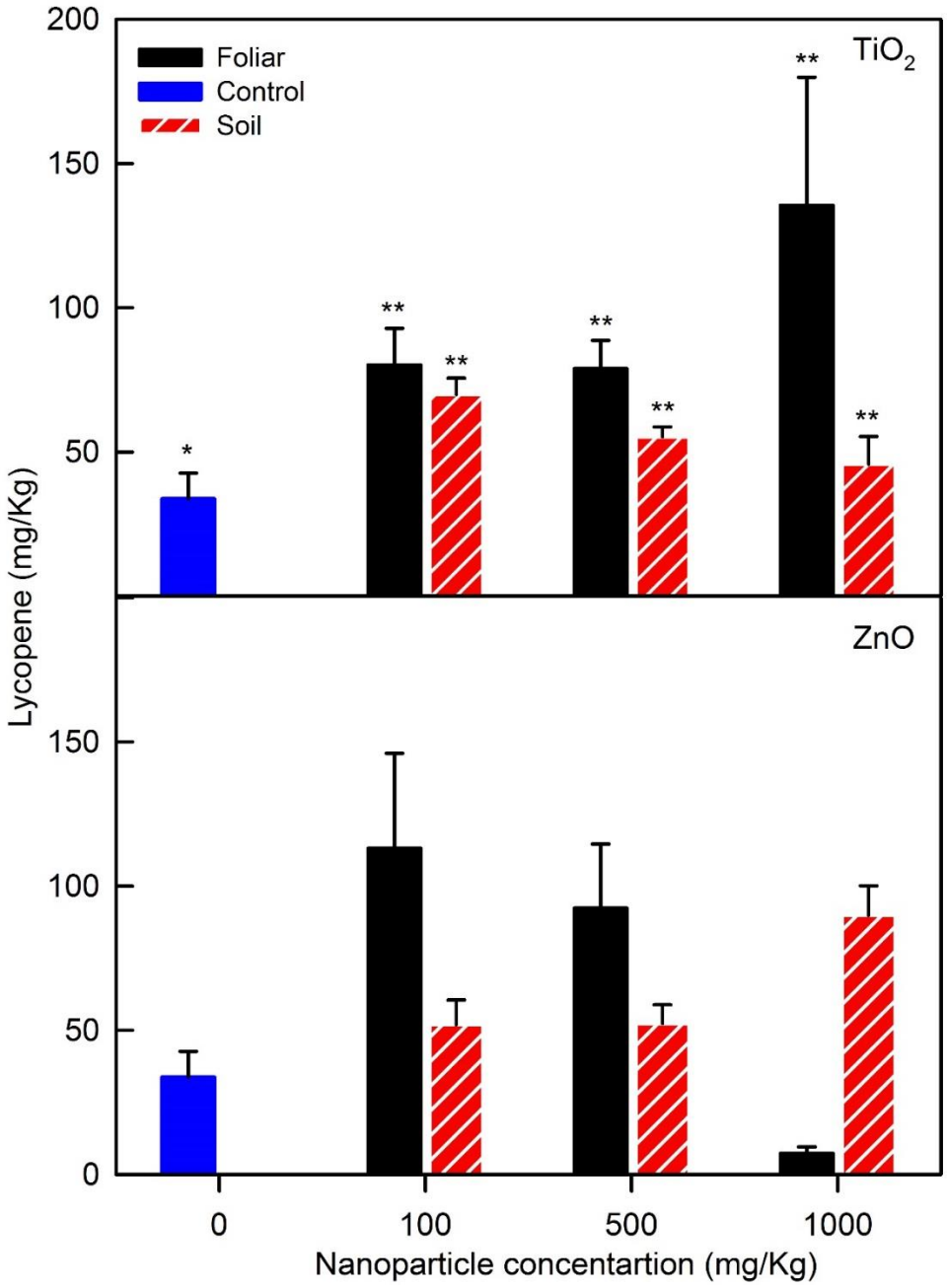

Fig. 5. Effect of TiO_2 and ZnO nanoparticles on lycopene content in tomato fruit. Error bar represents the standard deviation. *n = 4.* Asterisk(s) above bar demonstrate significant difference ($p < 0.05$).

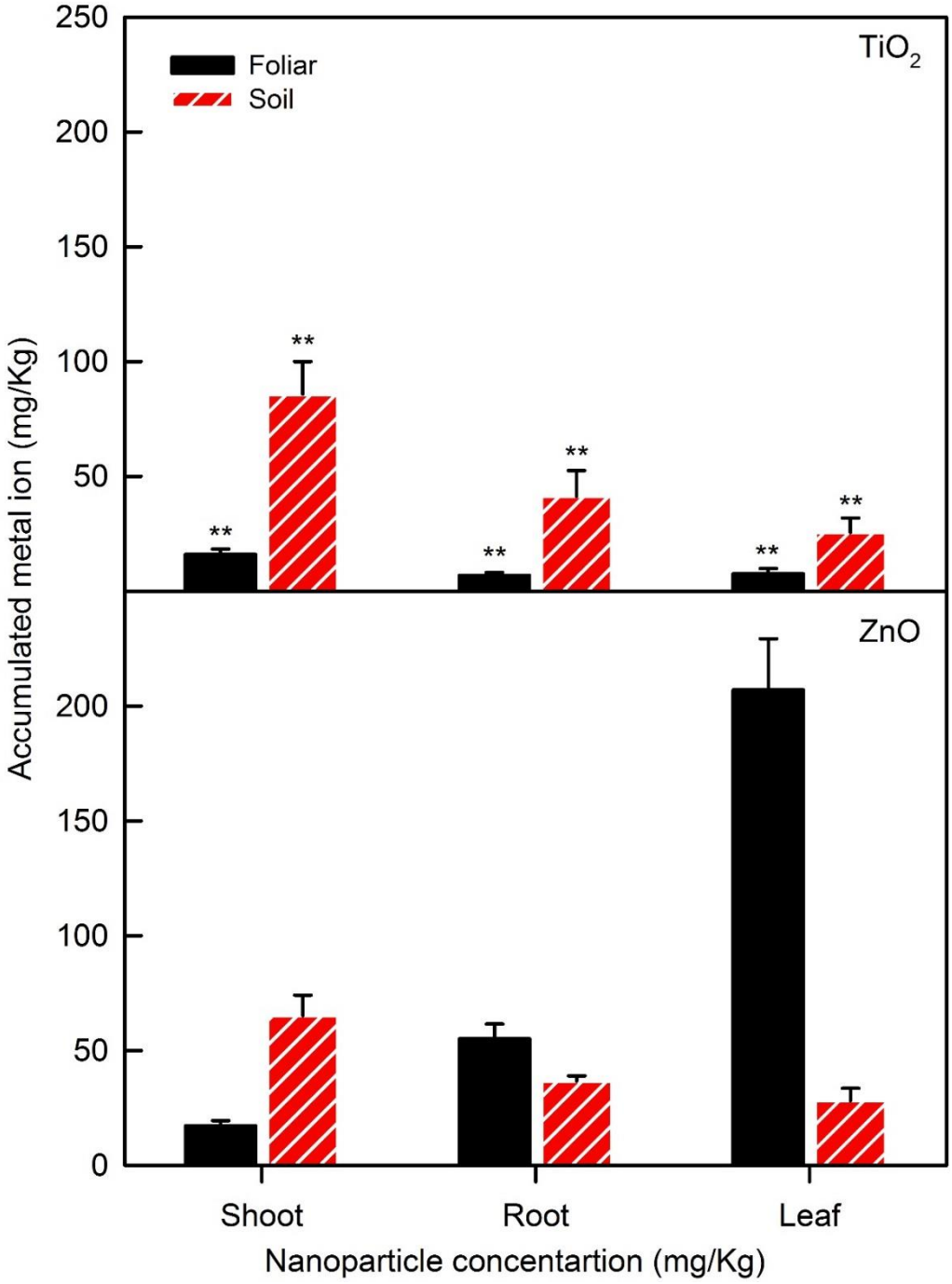

Fig. 6. Mobilization and accumulation of Ti and Zn among plant parts: accumulation of metal ion in stems, roots and leaves. Nanoparticles (250 mg/kg concentration) treated plant parts. Error bar represents the standard deviation. $n = 4$. Asterisk(s) above bar demonstrate significant difference ($p < 0.05$).

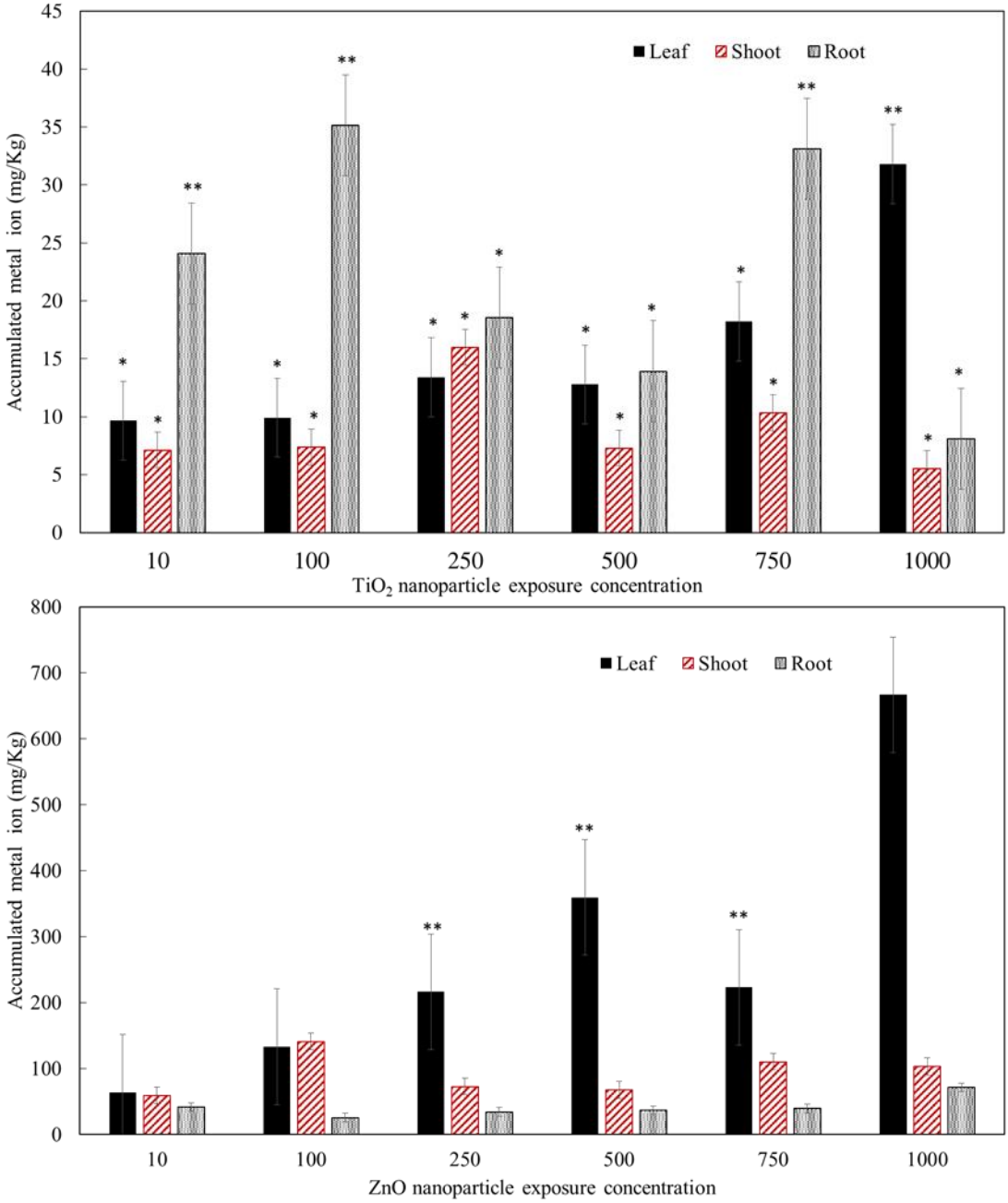

Fig. 7. Dose response changes in the concentration of Ti or Zn in the shoot, root and leaves at plant maturity stage. The representative figure shows the metal accumulation in the foliar exposure of TiO_2 or ZnO treated plants. Error bar represents the standard deviation. $n = 4$. Asterisk (s) above bar demonstrate significant difference ($p < 0.05$).

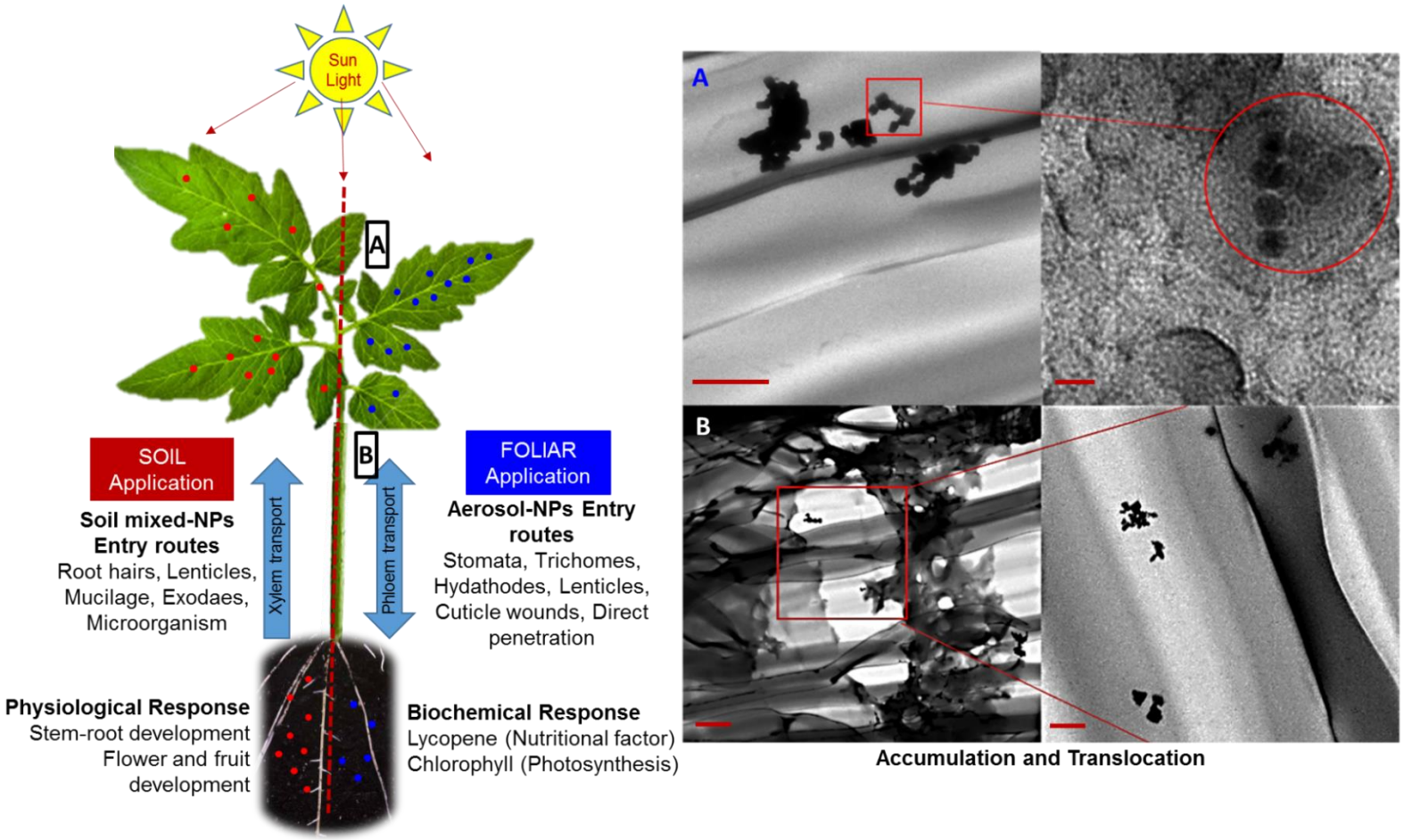

Fig. 8. Mechanistic understanding of nanoparticle uptake, translocation and accumulation helps explain change in tomato's physiological and biochemical responses. TEM micrograph of leaf (A) and stem (B) shows foliar application of TiO2 nanoparticles accumulation and translocation. Scale bar of inset A and B corresponds to 1 µ and magnified micrograph scale corresponds to 20 nm.